ACS Catalysis

Research Article

pubs.acs.org/acscatalysis

$CeMO_x$-Promoted Ketonization of Biomass-Derived Carboxylic Acids in the Condensed Phase

Ryan W. Snell and Brent H. Shanks*

Department of Chemical and Biological Engineering, Iowa State University, 1140L BRL, Ames, Iowa 50011, United States

Supporting Information

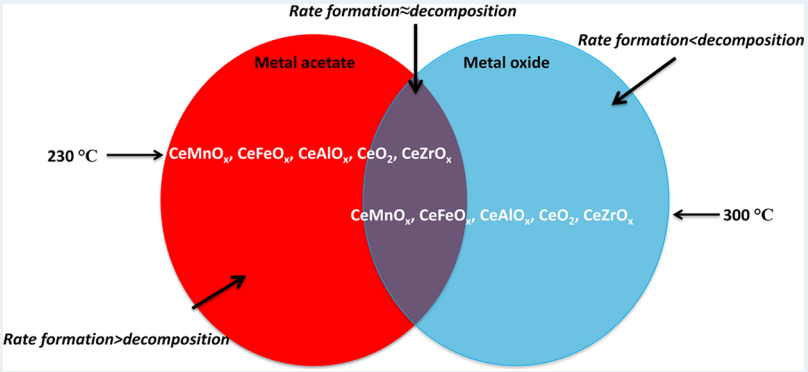

ABSTRACT: Ketonization of the model bio-oil compound acetic acid was performed in a toluene-solvent condensed phase using five different $CeMO_x$ catalysts. The catalysts were characterized using a number of different techniques both before and after reaction testing to gain understanding of how material traits influence their catalytic performance. A number of potentially important catalytic properties were found to be of little importance for the respective reaction. For instance, it was discovered that there was no direct correlation between prereaction surface area with activity for ketonization at high or at low temperatures. Furthermore, better reducibility of the oxide did not appear to correlate with improved ketonization rates. XRD of postreaction materials used at different temperatures demonstrated the reaction temperature regime influenced whether the crystal structure of the fresh mixed oxide was disrupted. The precise temperature regimes were different, depending on composition of the catalytic material. Catalytic activity was then found to be maximized when metal carboxylate formation and subsequent decomposition of the carboxylate were appropriately balanced.

KEYWORDS: *ketonization, mixed metal oxides, acetic acid, metal carboxylate, ceria*

1. INTRODUCTION

In the search for renewable sources of energy, there will inevitably be a need for liquid fuels. With the existing liquid fuel infrastructure in the trillions of dollars, it would be highly desirable to produce a completely compatible renewable substitute. Fast pyrolysis, involving the thermal breakdown of biomass in the absence of oxygen, has been examined as a potential starting point for the production of liquid fuels.[1−3] Unfortunately, the resulting liquid product from fast pyrolysis, bio-oil, has a low energy density due to a large number of highly oxygenated compounds and a pH of 2−3 due primarily to many small organic acids, making upgrading necessary.[1] Moreover, it would be preferable to perform this upgrading process in the condensed phase as many of the components of bio-oil are thermally unstable.

One reaction that would appear to be attractive for this upgrading application is ketonization, which involves coupling two carboxylic acids to form a ketone, CO_2, and H_2O. This reaction has already been probed in a number of manuscripts related to renewable fuel applications.[4−7] Biomass-related applications of ketonization are not new as the reaction was actually used to produce acetone industrially in the early 20th century from the decomposition of calcium acetate made through the mixing of lime and wood distillates.

A large number of metal oxide catalysts have been explored and found to be active for ketonization.[8] However, ceria-based catalysts are commonly believed to be among the best for the reaction.[9,10] Recently, mixed ceria−zirconia materials have found promising application as ketonization catalysts in the upgrading of biomass-derived intermediates to fuels.[11−13] While this mixed metal oxide is clearly effective in the reaction, there is little basis for determining why it would be uniquely better as a catalyst for ketonization relative to other potential mixed metal oxides. In fact, it is known that a number of $CeMO_x$ catalysts are active for the reaction. For instance, Nagashima et al. investigated many $CeMO_x$ oxides containing 10 mol % of the respective additional metal in the vapor phase ketonization of propanoic acid at 350 °C.[16] Catalysts containing Mn, Mg, or

Received: September 24, 2013
Revised: December 16, 2013
Published: December 20, 2013

Cu were found to be more active than pure ceria, with $CeMnO_x$ being the most active. Through further investigation of the $CeMnO_x$ catalysts, it was reported that increasing the Mn content to ~60% resulted in greater acid conversions.[14] Despite reports of mixed oxides being superior catalysts, there does not appear to be an understanding of why the activity enhancement occurs.

The mixing of ceria with various oxides is known to significantly alter the material properties of the oxide. For example, it has been found that the addition of zirconia to ceria allows for reduction of the bulk oxide to occur at lower temperatures.[15] A mixed ceria−alumina catalyst was found to have redox properties similar to those of mixed ceria-zirconia catalysts in that the bulk ceria was more easily reduced.[16] Properties like these may potentially be of importance in ketonization as it has been suggested that catalyst redox characteristics may play a role in the reaction mechanism.[14,17] Alternatively, recent work from our lab on ceria catalysts suggested that the ketonization reaction could proceed through the formation and subsequent decomposition of metal carboxylates.[18−20] If this was the case, ceria-based mixed oxides might be expected to have different activities due to the ease of formation and decomposition of a metal carboxylate intermediate.

Given these considerations, the current work focused on examining the performance of Ce-containing mixed metal oxide catalysts for the ketonization reaction in the condensed phase. The goal of the work was to identify what characteristics of the materials yielded the most active catalysts. Four $CeMO_x$ catalysts were prepared and characterized relative to CeO_2. All of the materials were used in the condensed-phase ketonization of the model bio-oil compound, acetic acid. Importantly, post-eaction characterization of all five catalysts was performed, and explanations for the differences in reaction performance for the various materials were proposed.

2. RESULTS AND DISCUSSION

2.1. Catalyst Prereaction Characterization. The coprecipitation synthesis of the four different mixed oxides and pure ceria resulted in materials that were subsequently named $CeZrO_x$, $CeAlO_x$, $CeMnO_x$, and $CeFeO_x$, and CeO_2. As given in Table S1 (Supporting Information), the surface areas of $CeZrO_x$, $CeFeO_x$, and $CeAlO_x$ were all larger than those with pure CeO_2. The surface area of the $CeZrO_x$ synthesized in this study (145 m^2/g) was slightly greater than that reported by Serrano-Ruiz (115 m^2/g) using a very similar synthesis technique.[21] Also provided in Table S1 (Supporting Information) are the XRF results for the materials that gave Ce/M molar ratios of about 1, which were close to the target values based on precursor addition.

XRD analysis of the materials only showed peaks related to the cubic cerium oxide phase (Figure 1). As can be observed in Figure 1, the mixed oxide materials had smaller crystallite sizes than the pure ceria catalysts as evidenced by the broadening of the diffraction peaks. Incorporation of the additional smaller cation into the ceria cubic lattice was also observed through shifting of the peak locations to higher 2θ values for the $CeMnO_x$ and $CeZrO_x$ materials, which has been reported previously for these types of materials.[21−24] SEM of the particles showed that the precipitated materials consisted of nonuniformly shaped particles (Figure S1, Supporting Information).

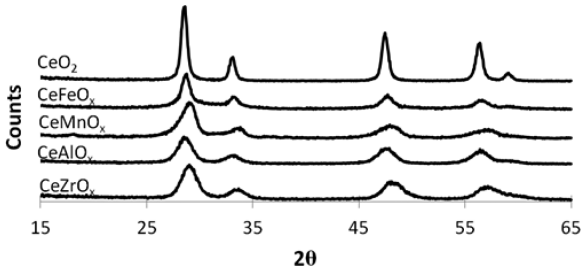

Figure 1. XRD profiles of the fresh mixed metal oxide catalysts.

TPR of the five catalysts showed significant differences in how easily the material could be reduced and whether these redox properties were maintained through at least two reduction cycles. As demonstrated in Figure 2, CeO_2 had

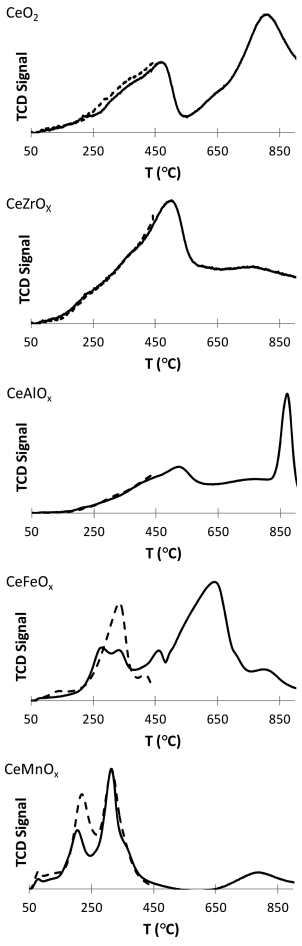

Figure 2. TPR of the $CeMO_x$ materials. The testing began with a reduction step up to 450 °C (- - -) followed by oxidation and a second reduction (—).

both low and high temperature reduction steps, which has commonly been reported to be due to surface and bulk oxygen removal, respectively.[25] Addition of other cations to CeO_2 clearly had significant impact on this reduction profile. Consistent with earlier reports, $CeZrO_x$ no longer gave a two-step reduction sequence, but instead, it appeared that the bulk and surface were reduced at the same time resulting in one large peak at ~450 °C.[15] $CeAlO_x$, $CeZrO_x$, and CeO_2 all seemed to maintain consistent reduction responses through at least two cycles, while $CeFeO_x$ and $CeMnO_x$ did not consume

dx.doi.org/10.1021/cs400851j | ACS Catal. 2014, 4, 512−518

as much H_2 during the second reduction event. $CeMnO_x$ reduction was similar to that reported by Chen et al. in that two peaks at ~250 and 350 °C occurred.[23] For both the manganese and the iron containing oxides, it must be kept in mind that significant reduction of Mn and Fe was likely occurring along with the $Ce^{4+} \rightarrow Ce^{3+}$ transition. For instance, the two-peak reduction with the $CeMnO_x$ sample may be due to consecutive reductions from a high oxidation state of Mn to one more reduced .[26]

XPS has been used for determining the cerium oxidation state present at the surface.[27] Nomenclature for the Ce 3d spectra as used here followed that proposed by Burroughs et al., which has now become standard.[28] The u‴ peak at a binding energy of 916.5 eV has been attributed to Ce^{4+} and is therefore used for calculation of the amount of this cerium oxidation state.[13] Shyu et al. found that the area % of this peak in relation to the entire Ce 3d spectra area followed a linear correlation with the % Ce^{4+} in the sample.[29] As can be seen in Figure 3, the

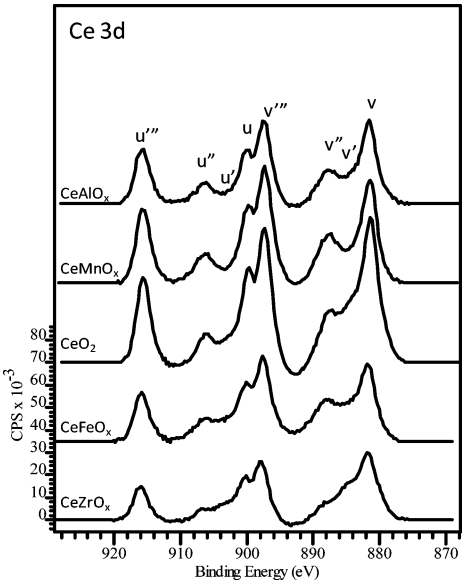

Figure 3. Ce 3d XPS spectra of the fresh materials, where u‴, v‴, u″, v″, u, and v peaks are attributed to Ce^{4+}, while the u′ and v′ peaks are related to Ce^{3+}.[13]

Ce 3d spectra for the five materials showed different levels of cerium reduction in the fresh materials. It was particularly evident for the $CeZrO_x$ material that the u‴ peak was decreased, while the v′ and u′ values increased significantly. This result was consistent with expectations as it is known that the addition of zirconia to ceria promotes vacancies charge balanced by the presence of Ce^{3+}.[30] The O1s spectra of the five materials are shown in Figure S2 (Supporting Information). While all of the materials gave peaks with broad shoulders at higher binding energies, the $CeAlO_x$ spectrum was unique in that at least two large distinct peaks were evident. While not observed in the XRD analysis, this two-peak result could likely be due to the separation of ceria and alumina phases. Therefore, the peak at the higher binding energy would be attributed to alumina with the remaining peaks due to oxygen present in ceria-aluminate and/or pure ceria.[31]

As shown in Figure 4, Raman spectra of the fresh materials all showed peaks at ~450−470 cm^{-1}, which is known to be due to the F2g Raman active mode common for ceria.[21,32,33] From

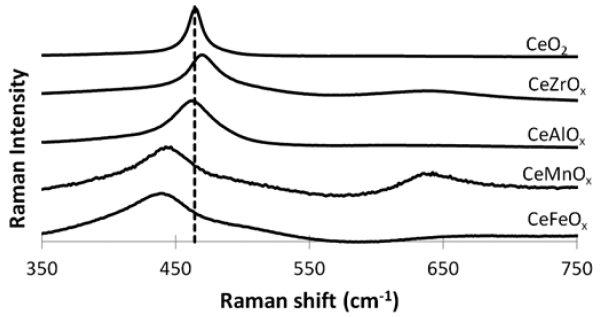

Figure 4. Raman spectra of the mixed metal oxide matierals with a laser power of 2.5 mW (CeO_2, $CeZrO_x$, and $CeAlO_x$) or 25 mW ($CeMnO_x$ and $CeFeO_x$).

Figure 4, it can be seen that the CeO_2 and $CeAlO_x$ peaks had similar Raman shifts, while the $CeZrO_x$ peak appeared to shift to the right. This blue-shift for $CeZrO_x$ has been reported elsewhere.[33,34] The red-shift seen for $CeMnO_x$ and $CeFeO_x$ may be due to heating of the sample by the higher laser powers used.[32] However, it is also known that red-shifts could be related to longer M-O bonds.[35]

2.2. Ketonization Reactions of Acetic Acid. Ketonization reactions of acetic acid resulting in the production of acetone, carbon dioxide, and water were performed in the condensed phase using stainless steel batch reactors. Initial reaction testing was performed at 230 °C using 0.2 g of catalysts. A catalyst was found to be necessary for the reaction to proceed, since a control run in the absence of any catalysts resulted in acetone molar yields under 0.1%. The catalyst runs were performed in duplicate with the results given in Figure 5.

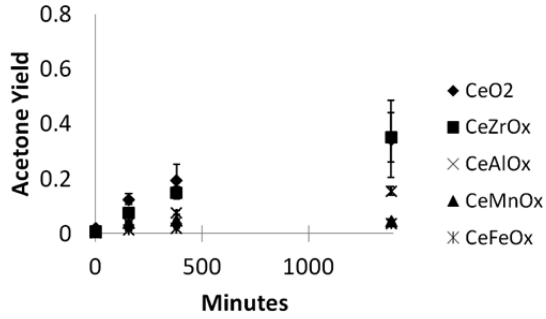

Figure 5. Acetic acid ketonization at 230 °C promoted by the $CeMO_x$ catalysts (0.2 g of catalyst and 1.0 g of acetic acid). Error bars are standard deviations from duplicate runs.

CeO_2 and $CeZrO_x$ were the most active catalysts giving similar acetone yields after ~23 h of reaction. $CeAlO_x$ gave an intermediate acetone yield, and $CeMnO_x$ and $CeFeO_x$ were the least active catalysts giving only ~4% yields at ~23 h.

Acetic acid ketonization was also performed at a higher temperature of 300 °C using a lower acid/catalyst weight ratio of 10. As shown in Figure 6, the results were quite different from those found at 230 °C. At the higher temperature, $CeMnO_x$ and $CeFeO_x$ were found to be the most active catalysts. Additional reactions were performed using a longer time of 45 min and a higher catalyst loading (acid/catalyst = 5). Under these conditions, $CeMnO_x$ and $CeFeO_x$ catalysts were the most active (Table S2, Supporting Information), in complete agreement with the reaction conditions used for Figure 6. Ceria-manganese oxide catalysts have been reported by Nagashima et al. to be more active than other mixed oxides

dx.doi.org/10.1021/cs400851j | ACS Catal. 2014, 4, 512−518

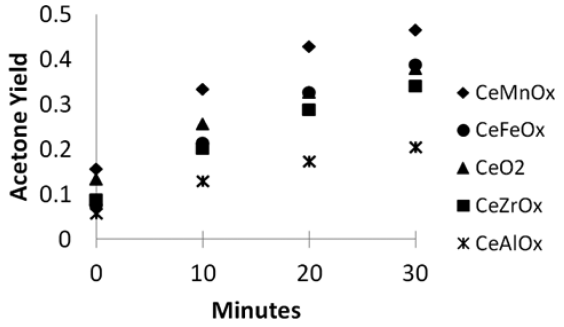

Figure 6. $CeMO_x$ activity in acetic acid ketonization at 300 °C (0.1 g of catalyst and 1.0 g of acetic acid).

when tested in the vapor phase ketonization of propanoic acid at 350 °C.[14]

To explore whether conversion could be achieved at even lower temperatures in the condensed phase, reaction testing was performed at 150 °C. Very little activity was observed for any of the materials with CeO_2 giving the greatest acetone yield of 1.2% after 24 h. However, there were differences in the amount of acetic acid lost during the reaction as the $CeMnO_x$ and $CeFeO_x$ materials were found to have acid loss of greater than 10%, while the other three materials all had acid disappearance at or below 6%.

2.3. Postreaction Catalyst Characterization. Characterization of the catalysts after reaction testing at 230 °C showed a number of interesting changes relative to the fresh materials. The SEM images revealed that during the course of reaction all of the materials other than $CeMnO_x$ formed a large number of whisker- or rod-shaped particles (Figure S3, Supporting Information), which demonstrated that significant particle restructuring occurred during the reaction. XPS of the five postreaction catalysts also showed significant reduction of the surface cerium for all of the catalysts (Figure 7). However, it was evident that CeO_2 was the least reduced with $CeFeO_x$ and $CeAlO_x$ having the most Ce^{3+} present. There have been reports

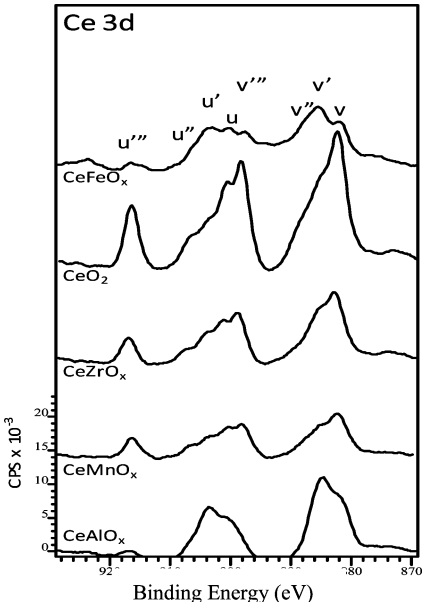

Figure 7. XPS of $CeMO_x$ catalysts after acetic acid ketonization at 230 °C for ~23 h.

of cerium reduction during the course of the ketonization reaction.[13,19,36]

XRD analysis of the catalysts after their exposure to the reaction at 150 °C, 230 °C, and 300 °C showed that depending on the material and on the reaction temperature the catalyst crystal structures had been modified. As shown in Figure S4 (Supporting Information), after 24 h of exposure to acetic acid at 150 °C both the $CeMnO_x$ and $CeFeO_x$ catalysts were significantly transformed from their original state, while the CeO_2, $CeZrO_x$, and $CeAlO_x$ catalysts all maintained their original fluorite structure. For the intermediate reaction temperature of 230 °C, all five of the catalysts were significantly altered with very little of the original crystallinity maintained (Figure 8). Reaction testing at 300 °C again resulted in a

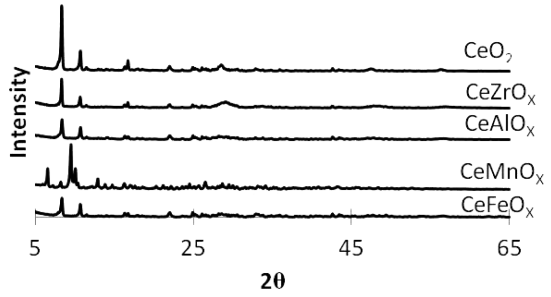

Figure 8. XRD of postreaction catalysts (230 °C, 23 h, 0.2 g of catalyst, and 1.0 g of acetic acid).

difference between the catalysts as seen in Figure 9. With this higher temperature reaction, only $CeMnO_x$ and $CeFeO_x$ were transformed, while the other oxides had XRD patterns similar to those before use in the ketonization reaction.

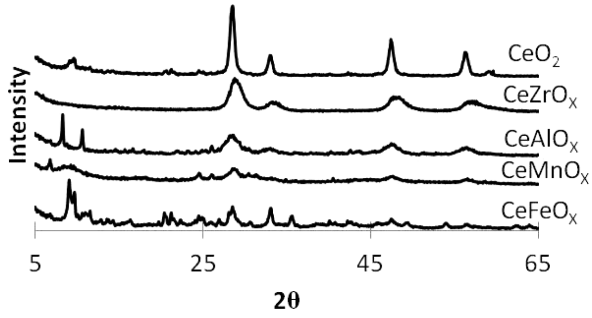

Figure 9. XRD of the postreaction catalysts (300 °C, 30 min, 0.1 g of catalyst, and 1.0 g of acetic acid).

2.4. Discussion. The metal oxides, Al_2O_3,[37] MnO_2,[8] Fe_2O_3,[38] and ZrO_x[39] have all been reported to be active ketonization catalysts by themselves, and as shown here, the addition of the respective metal into ceria altered a number of catalyst properties measured on the fresh materials. However, postreaction characterization suggested that many of these material characteristics could be eliminated as being of importance in the ketonization reaction under the conditions used in the current work. As shown in Table S1 (Supporting Information), the BET surface area was significantly different for the five catalysts, but the higher surface area values clearly did not correlate to greater acetone yields in reaction testing. This result implied that the ketonization was either not taking place solely on the surface of the materials or that significant

dx.doi.org/10.1021/cs400851j | ACS Catal. 2014, 4, 512−518

surface area was being lost during the course of the reaction due to reaction-induced restructuring.

TPR studies showed that addition of another cation into ceria created significant alterations in the reduction profile of the resulting material. Again, the TPR results examined in context of the reaction testing results did not show any clear trend between the ease of reduction and ketonization activity. Therefore, enhanced redox abilities could not be used to explain why mixed oxide catalysts were more active than pure ceria in some cases. The surface oxidation state of cerium in the fresh material did not have a significant correlation with catalytic activity. As shown in Figure 3, initially the mixed oxides contained different ratios of Ce^{3+}/Ce^{4+}. $CeMnO_x$ and $CeAlO_x$ appeared to have more Ce^{4+} than did $CeZrO_x$, and while $CeZrO_x$ was more active than both at 230 °C, $CeMnO_x$ was only more active at 300 °C.

XRD results for the materials after acetic acid ketonization displayed important differences between the materials as well as temperature-dependent results. At 150 °C, $CeMnO_x$ and $CeFeO_x$ underwent bulk restructuring, while CeO_2, $CeAlO_x$, and $CeZrO_x$ did not. This restructuring was likely due to a reaction of the acetic acid with the mixed metal oxide resulting in the formation of a mixed metal oxyacetate. The bulk carboxylate formation phenomenon has been reported previously for a number of different metal oxides.[37,40,41] In contrast, different interactions of the materials with the acetic acid reactant were observed after use at the intermediate reaction temperature of 230 °C. Here, the exposure to the acid resulted in the formation of bulk acetate for all five of the materials. Higher temperature reaction testing at 300 °C again showed that $CeFeO_x$ and $CeMnO_x$ preferred carboxylate formation, while CeO_2 and $CeZrO_x$ remained in the original oxide phase.

To our knowledge, this is the first finding of mixed metal oxides with cerium where bulk carboxylates were found to form during the ketonization of organic acids. There could be a number of reasons for bulk carboxylates not being reported previously. One is that mixed metal oxides have not been thoroughly examined after exposure to reaction conditions similar to those used in the current study. Importantly, the ketonization temperatures used here were lower than the 300−450 °C typically used for this reaction.[42] Alternatively, it is possible that the metal carboxylate formation was related to the use of a condensed phase during the ketonization reaction rather than the more typically examined vapor phase conditions. However, it is worth noting that our recent work with acetic acid ketonization using only ceria showed that bulk carboxylate formation was related to the reaction temperature rather than the phase in which the reaction was being performed.[19]

The formation of bulk carboxylates has been proposed to be of possible importance in the ketonization of carboxylic acids.[37,41,43] Yakerson et al. examined vapor phase ketonization of acetic acid with TiO_2, CeO_2, SnO2, ZrO_2, and BeO and suggested that these materials did not undergo bulk carboxylate formation unlike groups I and II carbonates or oxide catalysts.[43] To reconcile these differences, the authors proposed that ketonization proceeded through different mechanisms depending on the strength of the metal−oxygen bonds.[43] Pestman et al. reached a similar conclusion as they proposed oxides with weak M-O bonds promoted the reaction through a bulk decomposition mechanism, while oxides with strong M-O bonds catalyzed ketonization through a surface reaction.[37] Mekhemer et al. recently performed studies on the vapor phase ketonization of acetic acid using MgO catalysts and concluded that the basicity of the materials as well as the lattice energy influenced the formation of bulk acetates.[41] In this work, it was proposed that the reaction temperature played a role in determining if the reaction proceeded via bulk decomposition of a magnesium carboxylate or through surface-catalyzed mechanisms whereby at temperatures of >300 °C surface reactions began to become important, but at lower temperatures, the ketone produced resulted from bulk decomposition.[41]

In the current work, the results suggested that similar temperature-regime-dependent behavior was important. However, for the $CeMO_x$ materials examined there seemed to be different behaviors based on low, middle, and high temperature use rather than just the two regimes reported for MgO. The selection of the metal used for the $CeMO_x$ material dictated what temperature was required to access the various regimes. Comparison of the responses of the different materials suggested that at low temperatures with CeO_2, $CeAlO_x$, and $CeZrO_x$ there was no sufficient energy to break the M-O bonds and form carboxylates, whereas for $CeMnO_x$ and $CeFeO_x$, there was. At intermediate temperatures, there was an adequate amount of energy for carboxylate formation to overcome this barrier for all of the materials, and as such, the resulting metal acetate was stable, leading to transformation of the bulk oxide. At the higher temperature of 300 °C, there was sufficient energy to both form metal acetates and for them to decompose. These results were consistent with previously reported work that demonstrated cerium acetate decomposes at temperatures of about 300 °C with concomitant release of acetone.[44] Since the metal acetate can form and decompose at the higher temperature, the crystal structures of the materials remained intact. For the $CeMnO_x$ and $CeFeO_x$ materials, the carboxylate appeared to readily form at lower temperatures and then was stable at higher temperatures.

For all materials that were used at 230 °C for ∼23 h, their recalcination at 450 °C in air resulted in the reformation of their respective oxide crystal lattices as determined from XRD except for the $CeFeO_x$ material. For this material, there was an appearance of a new peak near a 2θ value of 36°. The location of the new peak was consistent with the formation of a second Fe_2O_3 phase upon recalcination. Therefore, the disruption of the mixed metal oxide crystal structure due to the formation of metal acetates could lead to irreversible bulk transformations leading to the phase segregation of constitutive metal oxides. Phase separation would expect to alter the properties of the catalytic material and could result in decreased performance at the desired reaction conditions.

To examine metal carboxylate formation and decomposition in more detail, TGA of the spent catalysts was performed (Figure 10). Decomposition of the 230 °C spent catalysts showed that $CeMnO_x$ and $CeFeO_x$ lost the most weight with $CeZrO_x$ and CeO_2 losing the least. These results suggested that the two former catalysts had greater acetate formation than did the two latter materials. Therefore, both the TGA and XRD results were consistent with the $CeMnO_x$ and $CeFeO_x$ more readily forming metal acetates, which were more stable, than for $CeZrO_x$ and CeO_2. The Raman spectroscopy results as shown in Figure 4 also helped support this supposition as the $CeZrO_x$ had its F2g peak shifted to larger wavenumbers in comparison to those of CeO_2, while $CeMnO_x$ and $CeFeO_x$ had smaller Raman shifts. This may be the result of stronger M-O bonds in

dx.doi.org/10.1021/cs400851j | ACS Catal. 2014, 4, 512−518

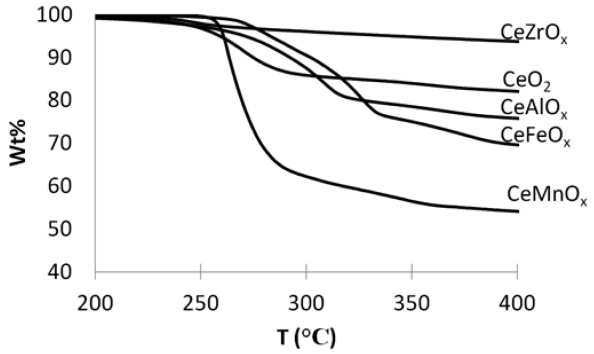

Figure 10. TGA results of postreaction catalysts used at 230 °C (~23 h, 0.2 g of catalyst, and 1.0 g of acetic acid).

the $CeZrO_x$ catalyst with weaker M-O bonding for $CeMnO_x$ and $CeFeO_x$. These weaker M-O bonds allow the materials to react more easily to the organic acid resulting in more facile formation of metal carboxylates.

Additionally, the SEM and XPS results showed changes in the materials occurring over the course of reaction testing in the intermediate temperature regime. For example, the formation of whiskers or rods, as seen in Figure S2 (Supporting Information), demonstrated that the macromorphology of the materials changed along with the crystal structure during use. The link between the morphological change and the formation of metal carboxylates would be consistent with a recent report by Go and Jacobson who found that during the formation of a mixed cerium gadolinium carboxylate, in their case a metal formate, the resulting product consisted of rod-shaped materials, which looked similar to the morphologies observed in the current work.[45] The reduction of cerium as found by XPS could be attributed to metal acetate formation as well. After use, the catalytic materials were dried in air prior to XPS characterization, which would readily convert Ce^{3+} present as Ce_2O_3 into Ce^{4+} through oxidation to CeO_2. However, the reduced Ce state persisted through drying, which would be consistent with the reduced Ce being present as Ce (III) acetate. While reduced Ce^{3+} was observed for all five catalysts tested at 230 °C, it was the most pronounced for $CeFeO_x$, $CeMnO_x$, and $CeAlO_x$, which were also the materials that had the greatest weight loss as determined by TGA. Therefore, the results were consistent with cerium reduction and carboxylate formation being linked.

Importantly, the activity of the different catalysts was linked to the different reaction temperature regimes. During intermediate temperature testing, CeO_2 and $CeZrO_x$ were more active than $CeFeO_x$ and $CeMnO_x$, while at higher temperatures, the reverse reactivity order occurred. As was reported in previous work that only examined CeO_2 as the catalyst,[19] the reaction activity results could be rationalized by a model in which metal carboxylates formed and then were decomposed to the ketone. In this model, there would then be a competition between the formation of metal carboxylate and its subsequent decomposition. The relative rates of the two events would be related to both metal oxide effects and reaction temperature. As shown here, bulk carboxylates could form at temperatures below where ketonization products were observed for some of the mixed metal oxides suggesting the energetics of the metal carboxylate formation were favored. At intermediate temperatures, the ketonization reaction occurred but was still limited to decomposition, which was why all of the materials were transformed into bulk carboxylates. In this temperature regime, catalysts that form less stable metal carboxylates and have stronger M-O bonds like $CeZrO_x$ and CeO_2 would be the most active. At higher temperatures where decomposition readily occurs, the reaction would be limited by the formation of the carboxylate so materials with weaker M-O bonds leading to easier metal acetate formation as was the case with $CeMnO_x$ and $CeFeO_x$ would be more active. The different behavior of the $CeAlO_x$ catalyst could be attributed to the existence of two different phases, one being alumina, which has been reported to be less active than ceria;[10] so this material would promote the reaction more similarly to a mixture of ceria and alumina.

3. CONCLUSIONS

A number of different ceria-based mixed metal oxide catalysts were synthesized and tested in the condensed phase ketonization reaction of acetic acid, which was chosen due to its relevance to bio-oil upgrading processes. Extensive characterization of the properties of the mixed metal oxides revealed that a number of catalyst properties normally believed to be of benefit, such as BET surface area and redox behavior, did not have a large influence on the reaction performance of the materials. Reaction studies coupled with postreaction characterization of the catalytic materials demonstrated that the ketonization reaction was found to proceed differently depending on which of three temperature regimes was used as well as which particular metal was introduced into the ceria framework. Importantly, the performance of the catalytic materials was correlated to the relative efficacy of forming metal acetates versus their decomposition to release a ketone. At intermediate temperatures, metal oxide catalysts such as $CeZrO_x$ and CeO_2, which did not as readily form metal carboxylates were found to be the most active, while at higher temperatures, the ability to form metal acetate such as with $CeFeO_x$ and $CeMnO_x$ was of benefit. Therefore, in the selection of a catalyst for a particular ketonization reaction system, it is useful to take into account the ease of formation for metal carboxylates as well as the temperature at which these intermediate compounds thermally decompose.

■ ASSOCIATED CONTENT

Supporting Information

Experimental section, SEM images of fresh and spent materials, and additional characterization results. This material is available free of charge via the Internet at http://pubs.acs.org.

■ AUTHOR INFORMATION

Corresponding Author

*E-mail: bshanks@iastate.edu.

Notes

The authors declare no competing financial interest.

■ ACKNOWLEDGMENTS

This work was funded by the National Science Foundation through the PIRE (OISE 0730227) and ERC (EEC-0813570) grants. Jim Anderegg (Ames Laboratory) was very kind in helping with the XPS results.

■ REFERENCES

(1) Czernik, S.; Bridgwater, A. V. *Energy Fuels* **2004**, *18*, 590−598S.
(2) Bridgwater, A. V. *Biomass Bioenergy* **2012**, *38*, 68−94.

(3) Wright, M. M.; Daugaard, D. E.; Satrio, J. A.; Brown, R. C. *Fuel* **2010**, *89*, S2−S10.
(4) Deng, L.; Fu, Y.; Guo, Q.-X. *Energy Fuels* **2009**, *23*, 564−568.
(5) Gärtner, C. A.; Serrano-Ruiz, J. C.; Braden, D. J.; Dumesic, J. A. *ChemSusChem* **2009**, *2*, 1121−1124.
(6) Gurbuz, E. I.; Kunkes, E. L.; Dumesic, J. A. *Green Chem.* **2010**, *12*, 223−227.
(7) Karimi, E.; Gomez, A.; Kycia, S. W.; Schlaf, M. *Energy Fuels* **2010**, *24*, 2747−2757.
(8) Glinski, M.; Kijenski, J.; Jakubowski, A. *Appl. Catal., A* **1995**, *128*, 209−217.
(9) Randery, S. D.; Warren, J. S.; Dooley, K. M. *Appl. Catal. A* **2002**, *226*, 265−280.
(10) Pulido, A.; Oliver-Tomas, B.; Renz, M.; Boronat, M.; Corma, A. *ChemSusChem* **2012**, *6*, 141−151.
(11) Kunkes, E. L.; Simonetti, D. A.; West, R. M.; Serrano-Ruiz, J. C.; Gartner, C. A.; Dumesic, J. A. *Science* **2008**, *322*, 417−421.
(12) Gaertner, C. A.; Serrano-Ruiz, J. C.; Braden, D. J.; Dumesic, J. A. *Ind. Eng. Chem. Res.* **2010**, *49*, 6027−6033.
(13) Gangadharan, A.; Shen, M.; Sooknoi, T.; Resasco, D. E.; Mallinson, R. G. *Appl. Catal., A* **2010**, *385*, 80−91.
(14) Nagashima, O.; Sato, S.; Takahashi, R.; Sodesawa, T. *J. Mol. Catal. A.: Chem.* **2005**, *227*, 231−239.
(15) Fally, F.; Perrichon, V.; Vidal, H.; Kaspar, J.; Blanco, G.; Pintado, J. M.; Bernal, S.; Colon, G.; Daturi, M.; Lavalley, J. C. *Catal. Today* **2000**, *59*, 373−386.
(16) Ilieva, L.; Pantaleo, G.; Ivanov, I.; Venezia, A. M.; Andreeva, D. *Appl. Catal., B* **2006**, *65*, 101−109.
(17) Hasan, M. A.; Zaki, M. I.; Pasupulety, L. *Appl. Catal., A* **2003**, *243*, 81−92.
(18) Snell, R. W.; Shanks, B. H. *Appl. Catal., A* **2013**, *451*, 86−93.
(19) Snell, R. W.; Shanks, B. H. *ACS Catal.* **2013**, *3*, 783−789.
(20) Snell, R. W.; Hakim, S. H.; Dumesic, J. A.; Shanks, B. H. *Appl. Catal., A* **2013**, *464*, 288−296.
(21) Serrano-Ruiz, J. C.; Luettich, J.; Sepúlveda-Escribano, A.; Rodríguez-Reinoso, F. *J. Catal.* **2006**, *241*, 45−55.
(22) Yao, M. H.; Baird, R. J.; Kunz, F. W.; Hoost, T. E. *J. Catal.* **1997**, *166*, 67−74.
(23) Chen, H.; Sayari, A.; Adnot, A.; Larachi, F. C. *Appl. Catal., B* **2001**, *32*, 195−204.
(24) Abdollahzadeh-Ghom, S.; Zamani, C.; Andreu, T.; Epifani, M.; Morante, J. R. *Appl. Catal., B* **2011**, *108−109*, 32−38.
(25) Yao, H. C.; Yao, Y. F. Y. *J. Catal.* **1984**, *86*, 254−265.
(26) Kapteijn, F.; Singoredjo, L.; Andreini, A.; Moulijn, J. A. *Appl. Catal., B* **1994**, *3*, 173−189.
(27) Trovarelli, A. In *Catalysis by Ceria and Related Materials*; Hutchings, G. J., Ed.; Catalytic Science Series; Imperial College Press, London, U.K., 2002.
(28) Burroughs, P. A. H.; Orchard, A. F.; Thornton, G. *J. Chem. Soc., Dalton Trans.* **1976**, *17*, 1686−1698.
(29) Shyu, J. Z.; Otto, K.; Watkins, W. L. H.; Graham, G. W.; Belitz, R. K.; Gandhi, H. S. *J. Catal.* **1988**, *114*, 23−33.
(30) Mamontov, E.; Egami, T.; Brezny, R.; Koranne, M.; Tyagi, S. *J. Phys. Chem. B* **2000**, *104*, 11110−11116.
(31) Sohal, R.; Lupina, G.; Seifarth, O.; Zaumseil, P.; Walczyk, C.; Schroeder, T. *Surf. Sci.* **2010**, *604*, 276−282.
(32) Fazio, B.; Spadaro, L.; Trunfio, G.; Negro, J.; Arena, F. *J. Raman Spectrosc.* **2011**, *42*, 1583−1588.
(33) Reddy, B. M.; Khan, A.; Yamada, Y.; Kobayashi, T.; Loridant, S.; Volta, J.-C. *J. Phys. Chem. B* **2003**, *107*, 11475−11484.
(34) Reddy, B.; Bharali, P.; Thrimurthulu, G.; Saikia, P.; Katta, L.; Park, S.-E. *Catal. Lett.* **2008**, *123*, 327−333.
(35) Masui, T.; Koyabu, K.; Minami, K.; Egawa, T.; Imanaka, N. *J. Phys. Chem. C* **2007**, *111*, 13892−13897.
(36) Rubinshtein, A. M.; Slinkin, A. A.; Yakerson, V. I.; Fedorovskaya, E. A. *Russian Chem. Bull.* **1961**, *10*, 2090−2092.
(37) Pestman, R.; Koster, R. M.; van Duijne, A.; Pieterse, J. A. Z.; Ponec, V. *J. Catal.* **1997**, *168*, 265−272.
(38) Kuriacose, J. C.; Jewur, S. S. *J. Catal.* **1977**, *50*, 330−341.
(39) Okumura, K.; Iwasawa, Y. *J. Catal.* **1996**, *164*, 440−448.
(40) Yamada, Y.; Segawa, M.; Sato, F.; Kojima, T.; Sato, S. *J. Mol. Catal. A: Chem.* **2011**, *346*, 79−86.
(41) Mekhemer, G. A. H.; Halawy, S. A.; Mohamed, M. A.; Zaki, M. I. *J. Catal.* **2005**, *230*, 109−122.
(42) Vivier, L.; Duprez, D. *ChemSusChem* **2010**, *3*, 654−678.
(43) Yakerson, V. I.; Fedorovskaya, E. A.; Klyachko-Gurvich, A. L.; Rubinshtei, A. M. *Kinet. Catal.* **1961**, *2*, 907−915.
(44) Arii, T.; Taguchi, T.; Kishi, A.; Ogawa, M.; Sawada, Y. *J. Eur. Ceram. Soc.* **2002**, *22*, 2283−2289.
(45) Go, Y. B.; Jacobson, A. J. *Chem. Mater.* **2007**, *19*, 4702−4709.